Clim. Past Discuss., 9, 5347–5389, 2013
www.clim-past-discuss.net/9/5347/2013/
doi:10.5194/cpd-9-5347-2013

Climate of the Past Discussions

Evaluation of seasonal climates of the Mediterranean and nothern Africa in the CMIP5 simulations

A. Perez-Sanz[1,2], **G. Li**[2], **P. González-Sampériz**[1], **and S. P. Harrison**[2,3]

[1]Pyrenean Institute of Ecology, (IPE)-CSIC, Avda. Montañana 1005, 50059 Zaragoza, Spain
[2]Department of Biological Sciences, Macquarie University, North Ryde, NSW 2109, Australia
[3]Centre for Past Climates and Department of Geography & Environmental Sciences, School of Archaeology, Geography and Environmental Sciences, (SAGES) University of Reading, Whiteknights, Reading, RG6 6AB, UK

Received: 7 August 2013 – Accepted: 4 September 2013 – Published: 17 September 2013

Correspondence to: A. Perez-Sanz (anaperez@ipe.csic.es, anpsanz@gmail.com)

Published by Copernicus Publications on behalf of the European Geosciences Union.

Abstract

We analyze the spatial expression of seasonal climates of the Mediterranean and northern Africa in pre-Industrial (*piControl*) and mid-Holocene (*midHolocene*, 6 ka) simulations from the fifth phase of the Coupled Model Intercomparison Project (CMIP5). Modern observations show four distinct precipitation regimes characterized by differences in the seasonal distribution and total amount of precipitation: an equatorial band characterized by a double peak in rainfall, the monsoon zone characterized by summer rainfall, the desert characterized by low seasonality and total precipitation, and the Mediterranean zone characterized by summer drought. Most models correctly simulate the position of the Mediterranean and the equatorial climates in the *piControl* simulations, but over-estimate the extent of monsoon influence and underestimate the extent of desert. However, most models fail to reproduce the amount of precipitation in each zone. Model biases in the simulated magnitude of precipitation are unrelated to whether the models reproduce the correct spatial patterns of each regime. In the *midHolocene*, the models simulate a reduction in winter rainfall in the equatorial zone, and a northward expansion of the monsoon with a significant increase in summer and autumn rainfall. Precipitation is slightly increased in the desert, mainly in summer and autumn, with northward expansion of the monsoon. Changes in the Mediterranean are small, although there is an increase in spring precipitation consistent with palaeo-observations of increased growing-season rainfall. Comparison with reconstructions shows that most models under-estimate the mid-Holocene changes in annual precipitation, except in the equatorial zone. Biases in the *piControl* have only a limited influence on *midHolocene* anomalies in ocean-atmosphere models; carbon-cycle models show no relationship between *piControl* bias and *midHolocene* anomalies. Biases in the prediction of the *midHolocene* monsoon expansion are unrelated to how well the models simulate changes in Mediterranean climate.

1 Introduction

The Mediterranean area, including southern Europe and northern Africa, is characterized today by a highly seasonal climate with summer drought and a wet season between October and March (Mehta and Yang, 2008). The generally low precipitation and marked seasonality gives rise to drought-adapted, sclerophyllous vegetation that is highly susceptible to wildfire during the dry season (Moreira et al., 2011). The Mediterranean region has experienced warming and increased drought in recent years (Camuffo et al., 2010; Hoerling et al., 2012; European Environment Agency, 2012) and has been identified as highly vulnerable to future climate changes (Giorgi, 2006). Model projections indicate large increases in temperatures and a reduction in mean annual precipitation (e.g. Meehl et al., 2007; Giorgi and Lionello, 2008; Nikulin et al., 2011), both of which would lead to large changes in vegetation cover and exacerbate wildfires (Amatulli et al., 2013). Given the high socio-economic costs of such changes, it is important to assess the reliability of model projections. Measures of how well the models simulate modern climate do not provide a measure of whether the simulation of climate changes is realistic. However, the evaluation of model performance in the geologic past does provide a way of making such an assessment (Braconnot et al., 2012; Schmidt et al., 2013).

The mid-Holocene (MH, 6000 yr BP) provides an opportunity to examine climate-model performance in the Mediterranean region. Palaeoenvironmental evidence suggests that the Mediterranean was wetter than today during the mid-Holocene. Lake levels across the region were higher than present (Kohfeld and Harrison, 2000; Magny et al., 2002; Roberts et al., 2008), indicating a more positive balance between precipitation and evaporation. Speleothem records also indicate increased precipitation compared to present (Roberts et al., 2011). The observed expansion of deciduous trees (Prentice et al., 1996; Roberts et al., 2004; Carrión et al., 2010) across the region indicates that there was a change in rainfall seasonality with increased summer rainfall (Prentice et al., 1996). The observed decrease of fires in lowland areas, coupled with

an increase in fires at higher elevations, is consistent with more humid conditions – which would suppress fires in already forested lowland regions but allow them to increase as forests expanded into higher elevation areas (Vannière et al., 2011). The changes in climate were spatially complex (Roberts et al., 2011), but pollen-based climate reconstructions (e.g. Cheddadi et al., 1997; Davis et al., 2003; Bartlein et al., 2011) show that most of the Mediterranean region was characterized by a year-round decrease in temperature and an increase in plant-available moisture.

Systematic comparisons with observations have shown that climate models are unable to reproduce the observed MH patterns of change in the Mediterranean. This was identified as a problem in atmosphere-only simulations of the mid-Holocene made during the first phase of the Palaeoclimate Modelling Intercomparison Project (PMIP1: see e.g. Masson et al., 1999; Guiot et al., 1999; Bonfils et al., 2004). Coupled ocean-atmosphere simulations made during PMIP2 were able to simulate the types of climate changes seen in the Mediterranean, but the geographic placement of these climate types, the spatial extent and the magnitude of the changes were not well captured (Brewer et al., 2007). In particular, the simulated changes in precipitation are small and insufficient to explain the observed expansion of deciduous forests in the region.

The Mediterranean climate involves a complex interaction between different processes acting at several different spatio-temporal scales (Xoplaki et al., 2003; Luterbacher et al., 2006; CLIVAR, 2010; Lionello, 2012). However, interannual variability in Mediterranean summer precipitation is linked to variability in the strength of the Afro-Asian monsoon system (Rodwell and Hoskins, 2001; Raicich et al., 2003; Gaetani et al., 2011). Analyses of climate model simulations of the present day suggest that Mediterranean summer precipitation is suppressed during years when the Afro-Asian monsoon system is strong. This results from intensification of the Hadley cell and enhanced subsidence in the subtropics (i.e. strengthening of the Azores High), leading to high pressure over the eastern Mediterranean which results in decreased rainfall (Gaetani et al., 2011). However, when monsoon intensification is accompanied by northward movement of the intertropical convergence zone, as model simulations indicate

occurred in the mid-Holocene (Braconnot et al., 2007a; Marzin and Braconnot, 2009), the Azores high is also displaced northeastward and weakened (e.g. Harrison et al., 1992). This has been shown to have a significant impact on precipitation in the eastern North America (Forman et al., 1995; van Soelen et al., 2012) and could potentially lead to increased summer rainfall in the Mediterranean region.

The PMIP2 simulations show a significant enhancement and northward expansion of the African monsoon during the Mid-Holocene in response to changes in insolation forcing (Braconnot et al., 2007a). However, comparisons with pollen-based estimates of the change in mean annual precipitation (Joussaume et al., 1999; Bartlein et al., 2011) show that the models underestimate the increase in precipitation by between 20 and 50 % (Braconnot et al., 2007a; 2012). Most models fail to produce a sufficient northward expansion of the monsoon. It is possible that this bias in the simulation of the African monsoon is linked to the failure to simulate the MH Mediterranean climate accurately, since larger shifts in the position of the monsoon are produced by models incorporating land-surface feedbacks and/or with higher spatial resolution (Levis et al., 2004; Wohlfahrt et al., 2004; Bosmans et al., 2012).

MH model simulations, made with the same models that are used for future projections, have been made as part of the fifth phase of the Coupled Model Intercomparison Project (CMIP5: Taylor et al., 2012). Kelley et al. (2012) have shown that the simulation of the seasonal cycle of precipitation in the Mediterranean region under modern conditions is reasonable, although as in earlier versions of the models the amplitude of the cycle is more muted than observed with too little rain in winter and too much rain in summer (Brands et al., 2013). However, evaluation of CMIP5 model performance against modern observations suggests that some aspects of the simulation of the Afro-Asian monsoons (see e.g. Monerie et al., 2012; Roehrig et al., 2013; Sperber et al., 2012) are improved compared to earlier versions of the models. However, there has been no assessment of whether this translates into an improved simulation of the MH monsoon climate, and thus given the dynamic links between the monsoon and Mediterranean precipitation, in MH Mediterranean climate changes.

In this study, we examine the performance of the CMIP5 models for modern and MH climates, and compare the simulated climates with modern and palaeo-observations. This allows us to assess whether biases in the control simulations influence the MH simulations and to investigate whether regional biases in the simulation of MH monsoon changes influence model performance in the Mediterranean.

2 Methods

We present analyses of the pre-Industrial (*piControl*) and MH (*midHolocene*) made by 12 coupled ocean-atmosphere models from the fifth phase of the Coupled Climate Modelling Intercomparison Project (CMIP5). In order to investigate whether biases in the control simulation influence the realism of the *midHolocene* climates, we first evaluate the *piControl* simulation. We use modern observations from the CRU TS3.1 data set, in the absence of climate reconstructions from northern African for the *piControl* interval. The *piControl* simulation is driven by boundary conditions appropriate for 1850AD, but comparisons with a subset of transient historical simulations show that the spatial patterns and magnitudes of seasonal climates are very similar. In order to evaluate whether models capture the spatial expression of specific seasonal patterns, we define a number of climate types using the modern observations and apply these definitions to delimit these climate types in the *piControl* and *midHolocene* simulations. We evaluate the *midHolocene* simulations using pollen-based palaeoclimate reconstructions. Comparisons of simulated and observed climates are based on the simulated precipitation both within climate zones and within geographic zones.

2.1 Data sources: CMIP5 simulations

We examine precipitation changes between a Mid-Holocene (*midHolocene*, 6000 yr BP) equilibrium simulation and a control simulation representing pre-industrial conditions (*piControl*) using 12 models from the fifth phase of the Coupled Modelling

Intercomparison Project (CMIP5). Both the *midHolocene* and *piControl* are equilibrium simulations. We use the *midHolocene* and *piControl* simulations in the CMIP5 (http://cmip-pcmdi.llnl.gov/cmip5/dataportal.html) archive as of 15 August 2012 (Table 1). Seven of these simulations are made with ocean-atmosphere (OA) models, and the other 5 models include an interactive carbon cycle (OAC). The *piControl* simulation has boundary conditions (insolation, greenhouse gas concentrations) appropriate for 1850 CE. The *midHolocene* experiment shows the response to changes in the seasonal and latitudinal distribution in insolation 6000 yr ago; greenhouse gas concentrations are set at *piControl* levels (for details of the experimental protocol see Taylor et al., 2012; Braconnot et al., 2012). To assess whether the *piControl* state differs from recent observed climates, we used outputs from a historical simulation (*historical*: 1850 to 2005 CE) available for 6 of the models. The *historical* simulation is forced by time-varying changes in solar, volcanic, and greenhouse gases (Taylor et al., 2012; Braconnot et al., 2012).

The output from each model was interpolated to a common grid (0.5°) using bilinear interpolation to facilitate comparisons and the calculation of zonal averages. Long-term mean monthly, seasonal, and annual precipitation values were obtained by averaging the last 100 yr of the *piControl* and *midHolocene* simulations, except in the case of HADGEM2-CC where only 35 yr of *midHolocene* simulated outputs are available. Long-term means of the six *historical* simulations were obtained by averaging the last 30 yr of each simulation. All averages were areally-weighted (by the area of the model grid cells).

2.2 Data sources: modern and mid-Holocene climate data

Observations of the modern climate are taken from the CRU TS3.1 data set (Harris et al., 2013), which provides monthly precipitation values on a 0.5° grid for the interval 1850 to 2006. We have created a monthly precipitation climatology using data from January 1961 through to December 1990. Zonal averages are constructed by areally-weighting the gridded values.

Bartlein et al. (2011) provide quantitative reconstructions of mean annual precipitation (MAP), expressed as anomalies from the present, from pollen and plant macrofossil records. The original site-based reconstructions were averaged to provide gridded values on a 2° × 2° grid, and differences between the site reconstructions within each grid were used to provide an estimate of reconstruction uncertainty (as a pooled estimate of the standard error). The data set provides mid-Holocene estimates of MAP anomalies for 62 cells (out of a possible 397 cells) within the area of interest (latitude: 0–45° N, longitude: 20° W–30° E).

2.3 Definition of climate regions

Precipitation regimes can be characterized by a combination of the form of the seasonal cycle, seasonal concentration, and magnitude. We determined these characteristics of modern precipitation (using the CRU TS3.1 data set) for zonally averaged 5° latitude bands between 0 and 45° N. The seasonal cycle of precipitation in each 5° latitude band was characterized according to the number of distinct rainfall peaks present in the 12-month precipitation climatology, using the R package "pastecs" to determine whether there was a significant "pit" or "peak" in any month. A pit or peak is considered significant if the probability of turning points occurring in a random series is < 0.05, given by:

$$(P(t) = 2/n(t-1)!(n-1)!)$$

where n is the number of observations at time t (Ibanez, 1982).

We calculated the total precipitation in each season (spring: March, April, May; summer: June, July, August; autumn: September, October, November; winter: December, January, February) and for the whole year. A measure of seasonal concentration was calculated following Kelley et al. (2013), where the magnitude of precipitation in each month is represented by the length of a vector in the complex plane and the direction of the vector represents the timing (with January set to 0°). The length of the mean vector divided by the annual precipitation provides an index of seasonal concentration

(C), where C is 1 when the precipitation is concentrated in a single month and 0 when it is evenly distributed throughout the year.

We applied these definitions to determine the position of different precipitation regimes in the *piControl* and *midHolocene* simulations. Comparison of the observed limits and those identified in the *piControl* allows us to examine (a) whether the models produce these distinctive precipitation regimes and (b) how well they simulate their placement independently of whether they simulate the correct magnitude of precipitation. Comparison of the *piControl* and *midHolocene* limits allows us to characterize shifts in precipitation regimes, again independent of changes in precipitation magnitude.

2.4 Analyses of the model simulations

We evaluate model performance for *piControl* simulation in two steps. First we examine whether the models reproduce the spatial extent of different precipitation regimes, and then we examine whether they reproduce the magnitude of total annual and of seasonal precipitation. Long-term means for the period 1961–1990 from the CRU TS3.1 data set (Harris et al., 2013) are compared with long-term averages for the last 100 yr of the *piControl*. The standard deviation (SD) of the observations provides a measure of the significance of the difference between observations and simulations. We examine the differences between simulated and observed climate for the latitude band corresponding to a given precipitation regime in the observations. We also compare the differences in the amount of precipitation for the geographic region identified as falling within a specific precipitation regime in each model, which may be less/more extensive than the region identified in the observations.

We also examine the change in precipitation in the mid-Holocene in two steps. First we identify the spatial extent of each precipitation regime in the *midHolocene* simulations and compare this with the spatial extent shown in the *piControl* simulation of the same model. This allows us to identify whether there have been shifts in the precipitation regimes. We then examine the magnitude of the precipitation change in the latitude

band characterized by a specific regime in both the *piControl* and the *midHolocene* simulations for each model. This allows us to identify whether there has been a change in precipitation in situ. We use the standard deviation of the *piControl* simulation for each model to determine whether the change between *midHolocene* and *piControl* is significant.

We examine whether the biases in simulated precipitation (both the bias in spatial extent of a given precipitation regime and the bias in the magnitude of the simulated precipitation) influence the simulated change in precipitation between *piControl* and *midHolocene*. The bias and anomaly values have been obtained firstly for discrete geographical zones (the zones characterized by different rainfall regimes today, as defined from the CRU data set) and secondly for the model-defined regions of these different rainfall regimes (e.g. the region where the simulated rainfall is of the monsoon type). We use linear regression to examine the relationship between precipitation biases and anomalies for all models, and for the OA and OAC classes of models.

The realism of the simulated change in precipitation (*midHolocene* – *piControl*) is assessed by comparing with reconstructions of mean annual precipitation (MAP) from the Bartlein et al. (2011) data set. Comparisons are made by averaging the simulated precipitation for the grid cells where there are observations within each 5° latitude band. There are sufficient data in most of the 5° latitude bands to make robust comparisons.

3 Results

3.1 Modern observed climate

The modern climate of the region can be divided into four distinct latitudinal zones, differentiated by marked differences in the seasonal distribution and amount of rainfall (Fig. 1). In the south, the equatorial band is characterized by high rainfall (~ 1800 mm) throughout the year (Fig. 2) but with peaks in precipitation in spring (~ 460 mm) and autumn (~ 600 mm) and less rainfall in summer. This pattern reflects the seasonal

migration north and south of the inter-tropical convergence zone. The "double-peak" rainfall pattern (hereafter DP) occurs between 0 to 5° N. The region further north (5–20° N) is characterized by summer monsoonal rainfall and dry winters. The amount of rainfall declines progressively from ca. 650 mm in summer (June, July, August) in the south to less than 100 mm in the north. The desert area (20–30° N) is characterized by low rainfall ($< 100\,mm\,yr^{-1}$). There is no pronounced seasonal differentiation in rainfall in the desert, although southern regions tend to have slightly more rain in summer than winter and northern regions slightly more rainfall in winter than summer. The Mediterranean zone (30–45° N) is characterized by higher rainfall, increasing from $200\,mm\,yr^{-1}$ in the south band to $780\,mm\,yr^{-1}$ in the north. The rainfall is concentrated in the winter half-year, with a pronounced summer drought.

3.2 PiControl simulations

These four rainfall regimes can generally be identified in the *piControl* simulations, although two of the models (CNRM-CM5, MRI-CGCM3) fail to reproduce the DP pattern in the equatorial zone. However, several models represent the spatial extent of the regimes poorly. Thus 5 out of the 12 models show monsoon penetration further north than observed (Fig. 3). Most models place the northern limit of the desert correctly, but two models (CSIRO-Mk3L-1-2, IPSL-CM5A-LR) show the area of low rainfall and low seasonality extending further north than observed.

Since there are no reconstructions of pre-industrial climate, we evaluate how well the models reproduce the magnitude of seasonal precipitation within each precipitation regime by comparing to observations for the period 1961–1990. Comparison of the *piControl* and *historical* simulations (SI, Fig. 1), for the six models where both runs are available, shows that differences in the simulated patterns and amount of precipitation between the two simulations are small. Differences between the two simulations are generally much smaller than the difference between the simulated and observed climate.

Comparison of the *piControl* with modern observations shows that most models fail to reproduce the magnitude of the precipitation (Fig. 4). Only two models (CSIRO-Mk3L-1-2, MPI-ESM-P) correctly reproduce the amount of rainfall in the DP band, while 6 models overestimate the rainfall by between 350 and $790\,mm\,yr^{-1}$. Although some models overestimate the amount of precipitation in every season, the positive biases are largest in spring (75–290 mm), autumn (90–325 mm) and winter (50–290 mm). Only two models (GISS-E2-R, CNRM-CM5) simulate the correct magnitude of mean annual precipitation in the monsoon zone. Seven models underestimate, and three models overestimate, the mean annual rainfall in the monsoon zone. The bias ranges from 280 mm less than observed to 270 mm more than observed. Models that underestimate the total amount of rainfall in the monsoon zone (e.g. BBC-CSM1.1, CSIRO-Mk3L-1-2, HadGEM2-CC, HadGEM2-ES, IPSL-CM5A-LR, MPI-ESM-P and MRI-CGCM3) do so because of simulating too little precipitation in summer and autumn, i.e. because the simulation of the monsoon is too weak. However, models that overestimate the total precipitation in this zone (e.g. CCSM4, CNRM-CM5, CSIRO-Mk3-6 and MIROC-ESM), generally overestimate the rainfall in all seasons of the year. Seven models simulate too much precipitation in the desert zone ($10\text{-}55\,mm\,yr^{-1}$), with too much rainfall in spring, summer and autumn. Given that the desert zone is by definition confined to regions with < 100 mm precipitation, the overestimation of rainfall in this zone is large. Four models underestimate the Mediterranean precipitation (by between 35 to $90\,mm\,yr^{-1}$), because of underestimation of the autumn and winter rainfall, although they overestimate the summer rainfall. However, the IPSL-CM5A-LR and GISS-E2-R models overestimate total precipitation in this region: GISS produces too much rainfall in spring (45 mm), summer (100 mm) and autumn (60 mm), while IPSL-CM5A-LR simulates too much rainfall (130 mm) in summer only. Comparison of results from models that correctly simulate the location of each regime (compared to the observations) and those in which the area characterized by a given regime is too extensive or too small, show that the biases in simulated precipitation are not related to whether models reproduce the spatial location of each regime correctly.

3.3 Mid-Holocene simulation

The location of the DP regime does not change between the *piControl* and *midHolocene* simulations of most (9) of the models (Fig. 5). The two models (CNRM-CM5, MRI-CGCM3) that failed to simulate a DP pattern in the equatorial zone in the *piControl*, nevertheless simulate this pattern in the *midHolocene* experiment. However, in the IPSL-CM5A-LR *midHolocene* simulation, the precipitation in the equatorial zone is more monsoon-like than in the model's *piControl* simulation. Most of the models (6) show no change in the northern limit of the monsoon; four models (CCSM4, IPSL-CM5A-LR, MRI-CGCM3, CNRM-CM5) show a northward displacement of the northern limit of the monsoon, while two models (BCC-CSM1.1, MRI-CGCM3) show a southward displacement of the northern limit of the monsoon as a result of southward expansion of the desert regime. Only two models (BBC-CSM1.1, MRI-CGCM3) show a northward displacement of the northern limit of the desert zone. Thus, in most of the *midHolocene* simulations, the desert regime occupies either a similar (5 models) or a slightly contracted area (4 models) compared to the *piControl*. Only one model (GISS-E2-R) shows a southward expansion of the Mediterranean precipitation regime; otherwise, this zone occupies the same position as in the *piControl* simulations.

We necessarily confine our comparisons of the magnitude of changes within each precipitation regime to those models that simulate a given regime in both the *piControl* and *midHolocene* simulations. The changes in the DP regime are not consistent and in general do not exceed the variability shown by the *piControl*. Only two models (CSIRO-Mk3-6-0, MIROC-ESM) show a significant reduction in precipitation (of 200 and 250 mm, respectively) in the *midHolocene* compared to the *piControl* (Fig. 6; Table 2). In the case of the CSIRO-Mk3-6-0 model, this is the result of a large decrease in autumn precipitation but in the case of the MIROC-ESM the decrease is concentrated in the spring. The monsoon zone is characterized by a significant increase in precipitation, except in the case of the CSIRO-Mk3-6-0 model. The anomalies range from +50 to +200 mm yr^{-1}, reflecting large increases in summer (15–140 mm) and autumn

(20 to 250 mm) rainfall. Changes in winter and spring precipitation are not significant. Most models show an increase in mean annual precipitation in the desert regime (5 to 35 mm) as a result of increased summer and autumn rainfall, but the change only exceeds *piControl* variability in three cases (CCSM4, GISS-E2-R and MIROC-ESM). Most of the models (11) show an increase in mean annual precipitation (10 to 75 mm) in the Mediterranean regime, although this increase only exceeds the *piControl* variability in the case of the GISS-E2-R model. The simulated increase in mean annual precipitation in the GISS-E2-R model results from an increase in spring, summer and autumn and a negligible change in winter. All of the models show an increase in spring precipitation, and two models (IPSL-CM5A-LR, HADGEM2-CC) show an increase in summer rainfall accompanied by either a small increase or no change in winter.

3.4 Comparison of *midHolocene* simulations and mid-Holocene observations

Reconstructions of the change in mean annual precipitation in the mid-Holocene (Fig. 7) show somewhat drier conditions (ca. 40 mm yr^{-1}) in the equatorial zone (0–5° N), an increase in precipitation of between 300–400 mm yr^{-1} between 10–30° N, and an increase of between 100–150 mm yr^{-1} in the Mediterranean (35–45° N). The simulated changes lie within the observed range between 0–5° N, with only 3 of the models lying outside the 25–75 % range. Several models simulate changes within the range of the observed increase in precipitation between 10–15° N (e.g. MRI-CGCM3, HADGEM2-CC, HADGEM2-ES, MIROC-ESM, IPSL-CM5a_LR, CCSM4). However, none of the models simulates the observed increase in precipitation (mean of ca. 390 mm yr^{-1}) between 15–30° N or indeed simulate changes within the range of the observations (Fig. 7). This is true even in the southernmost zone (15–20° N), although in this zone some of the models (e.g. MIROC-ESM) simulate a change of ca. 50 % of the observed mean change in precipitation. Models underestimate the reconstructed change in precipitation in the Mediterranean zone (35–45° N), although most models lie within the extremes of the observational range. The highest simulated

change in precipitation is ca. 50 mm yr^{-1} (GISS-E2-R) compared to the reconstructed mean change of between 100–150 mm yr^{-1}.

3.5 Comparison between bias and anomaly

Comparison of the *piControl* bias and *midHolocene* anomaly suggests that model performance in the control simulations directly affects model performance in the *midHolocene* simulations in the DP, desert and Mediterranean regions (Fig. 8). In the DP region, there is a significant negative significant correlation (Fig. 8, all models, black line: slope = −0.23, $R^2 = 0.74$, $p = 0.0$) between the bias and the anomaly: models that overestimate precipitation in the *piControl* show the largest reductions in precipitation in the *midHolocene* simulations (e.g. BCC-CSM1.1, CSIRO-Mk3-6-0 and MIROC-ESM). The overall relationship is driven by the OAC simulations (red line: $R^2 = 0.88$, $p = 0.02$); the slope for the OA models is not significant (blue line; $R^2 = 0.37$, $p = 0.2$). Indeed, as examination of these relationships in model-defined DP regions shows, the negative relationship shown by the OA models in the 0–5° N is driven by the two models that simulate monsoon-like regimes in this zone in the *piControl*.

There is no relationship between the *piControl* bias and the *midHolocene* anomaly in the monsoon zone (Fig. 8), whether this is defined geographically (slope = 0.00, $R^2 = 0.0$, $p = 0.98$) or using the model-based regimes (slope = 0.08, $R^2 = 0.05$, $p = 0.49$). Thus, the ability to simulate the correct magnitude of modern precipitation appears to have no influence on the magnitude of the response of the monsoon to changed forcing. However, the OA and OAC models appear to show opposite tendencies: the OA models show a weakly positive relationship between the bias and the anomaly (models that simulate less rainfall than observed in the *piControl* produce smaller MH anomalies) whereas the OAC models show a (very) weakly negative relationship.

There is a significant positive correlation between the *piControl* bias and *midHolocene* anomaly in the desert region (Fig. 8). This is true whether the region is

defined geographically (slope = 0.32, $R^2 = 0.58$, $p = 0.01$) or using the model-defined desert regimes (slope = 0.32, $R^2 = 0.48$, $p = 0.02$). Models that produce a reasonable simulation of modern rainfall in this region fail to produce a significant enhancement in the *midHolocene* simulation (CSIRO-Mk3L-1-2, HadGEM2-CC, IPSL-CM5A-LR) whereas models that are too wet in the *piControl* produce large changes in the *midHolocene* (CCSM4, GISS-E2-R and MIROC-ESM). However, these relationships are driven by the OA simulations; the OAC simulations do not show any significant relationship between the *piControl* bias and the *midHolocene* anomaly.

There is also a significant positive correlation between bias and anomaly in the Mediterranean region (Fig. 8), whether the region is defined geographically (slope = 0.14, $R^2 = 0.58$, $p = 0.01$) or using the model-defined regimes (slope = 0.15, $R^2 = 0.48$, $p = 0.02$). Models that underestimate precipitation in this zone in the *piControl* show only small increases in the *midHolocene* (BCC-CSM1.1, CCSM4 and MPI-ESM) while models with positive bias (GISS-E2-R and IPSL-CM5A-LR) produce larger changes in precipitation. However, the relationship for the OAC simulations is again non-significant.

Even in those regions where there are significant relationships between *piControl* bias and the *midHolocene* anomaly, the R^2 value ranges from 0.48 to 0.75. Thus, the bias in the *piControl* is not the only factor that determines whether the simulated magnitude of the MH climate change is correct. Furthermore, biases in the *piControl* appear to have less (or no) influence on the simulated *midHolocene* anomaly in the OAC simulations, except in the DP zone.

4 Discussion

Our analyses suggest that the CMIP5 models fail to reproduce key aspects of both the modern and MH climate of the northern Africa and Mediterranean region. Although the models generally reproduce the four characteristic seasonal patterns of precipitation, they do not always simulate these patterns in the correct place. They also tend

to underestimate the magnitude of seasonal changes in precipitation. For example, they underestimate the amount of winter rainfall and overestimate the summer rainfall in the Mediterranean region. This is consistent with previous analyses of Mediterranean climates in both the CMIP3 (Giorgi and Lionello, 2008) and CMIP5 (Kelley et al., 2012) simulations. The models overestimate the precipitation in the DP zone, again a feature identified from previous analyses (Roehrig et al., 2013). Previous analyses of the CMIP5 models (e.g. Roehrig et al., 2013; Brands et al., 2013) have suggested that there is a tendency for models to underestimate precipitation in the Sahel zone. While our analyses confirm this, with 8 out of 12 models showing less summer precipitation than observed, some of the models (e.g. CSIRO-Mk3L-1-2, BCC-CSM1.1) show a distinct improvement when the comparison is made between regions defined by precipitation regimes rather than geographically (Fig. 4). Furthermore, the temporal interval used for comparison also plays a role: MIROC-ESM, for example, simulates summer precipitation correctly but annual rainfall is too large because the simulated monsoon season is too long. Our evaluations are based on the assumption that the difference in climate between the *piControl* (1850 AD) and the 1961–1990 modern climatology is small. Comparisons of the *piControl* and *historical* simulations (Fig. S1, Supplement) for a sub-set of the models appear to support this assumption: the differences between the simulations are smaller than the difference between the simulated and observed climates. There is no synthesis of data for the pre-industrial era from northern Africa, but data from the Mediterranean region does not suggest substantial differences (e.g. Davis et al., 2003).

The models produce a northward shift and amplification of monsoon precipitation in the MH in response to insolation forcing. While the broad-scale patterns of change are consistent with the observations, the magnitude of these changes is significantly underestimated (Fig. 7). The failure to simulate a sufficiently large expansion of the African monsoon has been a major criticism of previous generations of climate models (Joussaume et al., 1999; Coe and Harrison, 2002; Braconnot et al., 2007a; Brayshaw et al., 2011; Zhao and Harrison, 2011; Braconnot et al., 2012). Comparisons between

CMIP5 and PMIP2 models (Fig. 9) show that the two ensembles are indistinguishable in terms of simulated changes over this study region. Global comparisons of these two sets of simulations (e.g. Harrison et al., 2013) appear to confirm that the CMIP5 models are no better at simulating climate changes than previous generations of models.

Our MH model evaluation is based on pollen-based reconstructions of mean annual precipitation. Although increase in monsoon precipitation is large (300–400 mm between 5 and 30° N) and spatially coherent, there are some zonal bands where the number of reconstructions is limited (see Fig. 7). However, other sources of palaeoenvironmental data, including vegetation (Hoelzmann et al., 1998; Prentice et al., 2000; Watrin et al., 2009; Niedermeyer et al., 2010), lake-level reconstructions (Kohfeld and Harrison, 2000; Tierney et al., 2011), and archaeological evidence (Kuper and Kröpelin, 2006; Dunne et al., 2012), show that the magnitude of the reconstructed precipitation changes in these zones is plausible. Furthermore, the reconstructions of climate conditions in the Mediterranean region are based on a much larger number of individual data points (Bartlein et al., 2011). Thus, the discrepancies between the model simulations and the observations are not simply a result of lack of information.

The simulated increase in mean annual precipitation in the Mediterranean region is small and, in comparison with the variability already present in the *piControl*, is not significant. However, although just half of the models show an increase in summer, all of them show an increase in precipitation in spring and some of them also show an increase in autumn. Thus, some of the models produce an increase in growing season moisture that, although too small, is consistent with the expansion of deciduous forest in this region during the mid-Holocene. Temperate deciduous forests occur in mid-latitude regions with > 700 mm of annual precipitation, spread throughout the year (see Harrison et al., 2010) Temperate deciduous forest occurs, for example, around Lake Banyoles in eastern Spain, where mean annual precipitation is ca. 800 mm and nearly half of this falls in spring and summer (Soler et al., 2007). According to the mid-Holocene simulations for the Mediterranean area, the largest increase in growing-season precipitation is ca. 30 mm in spring and 40 in summer (GISS-E2-R and HadGEM2-CC

respectively), and the overall change in mean annual precipitation is < 75 mm (GISS-E2-R). This is less than the increase required for deciduous trees to grow. Nevertheless, these simulations point to mechanism that could help to explain the observed vegetation changes in the Mediterranean. Furthermore, if the absence of a significant increase in summer rainfall in the Mediterranean is linked to underestimation of the northward migration of the African monsoon, then improvements in the simulation of monsoonal changes should also lead to a more realistic simulation of Mediterranean climate.

We have shown that there is a significant relationship between the bias in the control simulation and the magnitude of the simulated MH changes in precipitation for the DP, desert and Mediterranean zones, although no such relationship is present in the monsoon zone. However, the relationship in the desert and Mediterranean zones is only apparent in the OA models; the *piControl* bias does not seem to affect the *midHolocene* anomaly in the OAC models. The OA models also show a weakly positive (though non-significant) relationship between *piControl* bias and *midHolocene* anomaly in the monsoon region. Thus, the apparently significant relationships between bias and anomaly found when considering all the models are not a consistent feature of these simulations. Even in the DP, desert and Mediterranean zones, the bias in the OA *piControl* simulations only explains part of the variability in simulated climate changes. Previous studies have also had difficulties in finding consistent relationships between control biases and MH changes in precipitation. Comparison of control and MH atmosphere-only simulations made in the first phase of the Palaeoclimate Modelling Intercomparison Project (PMIP1) showed that inter-model differences in the position of the intertropical convergence zone in the control simulation was reflected in the inter-model differences of its position in the MH simulation (Joussaume et al., 1999). However, there was no clear relationship between the amount of precipitation in the control and the increase in precipitation in the MH (Braconnot et al., 2002). Braconnot et al. (2007b), analysing OA simulations from PMIP2, showed that the relationship between the simulated precipitation in the control to the ratio of the change in precipitation between MH and control was

negative: models that simulated very little rainfall tended to produce larger changes at the MH. However, this relationship was clearly driven by only three models, and the remaining models show no trend between the precipitation in the control simulation and the ratio of change in the MH. Thus, this seems to be consistent with our analyses. It is hard to escape the conclusion that improvements to the simulation of modern climate (see e.g. Haerter et al., 2011) will not guarantee that climate changes will be correctly simulated.

In this study, we have analysed the realism of simulated climates both in terms of climate regimes and by comparing specific geographic bands. The use of climate regimes places less stringent requirements on model performance, allowing an assessment for example of whether a model can simulate changes in seasonality independent of location. One reason for adopting this approach is the concern that model resolution, particularly in regions of complex topography, could affect geographic patterning (see e.g. Brewer et al., 2007). However, it can be difficult to find objective criteria for the definition of these climate regimes. Although we have been able to distinguish DP from monsoon, and monsoon from desert, climates solely on the basis of precipitation seasonality, it is not possible to use this type of criterion to distinguish desert and Mediterranean climates. Brewer et al. (2007) used *k* means clustering to define climate regimes in Europe. Although this is an approach that needs to be further explored, it involves some arbitrary decisions about the climate variables used for clustering as well as the number of clusters considered.

Many of the large-scale features characteristic of projected climate changes are a feature of past climate changes, and comparison with palaeo-observations shows that current models reproduce these features in a realistic way (e.g. Braconnot et al., 2012; Izumi et al., 2013; Schmidt et al., 2013; Li et al., 2013). Models, as we confirm here for northern Africa and the Mediterranean region, are also able to simulate precipitation regimes and shifts in these regimes in a realistic way (Joussaume et al., 1999; Braconnot et al., 2007a; Brewer et al., 2007). However, there are still important discrepancies between the simulated and observed magnitude of changes in precipitation, despite

the increasing complexity and resolution of the CMIP5 models compared to earlier generations of models. Given that the ability to simulate the magnitude of MH changes in seasonal climates does not appear to be systematically related to biases in the control simulations, focusing on improving the simulation of modern climate will not ensure that future projections or retrodictions of the climate of the Mediterranean and northern Africa will be more reliable. This is of concern given the environmental problems associated with recent climate changes in the Mediterranean and the importance of monsoonal rainfall for agriculture in northern Africa.

5 Conclusions

The CMIP5 models fail to reproduce key aspects of both the modern and MH climate of the northern Africa and Mediterranean region, including the correct geographical location of zonal precipitation regimes in the pre-industrial simulation and the magnitude of MH changes in these regimes.

Although biases in the OA simulations explain part of the variability in simulated climate changes, a similar relationship is not found for the OAC simulations. Thus overall, biases in the control simulations cannot explain the failure to reproduce MH changes in precipitation.

As in previous generations of model simulations, the CMIP5 simulations underestimate the northward shift and the magnitude of observed changes in the northern African monsoon.

In the Mediterranean region, the simulations show a tendency for increased growing-season precipitation. Such a shift is required to explain observed vegetation changes in this region in the MH, but the simulated shift is much too small. We speculate that this is linked to the underestimation of changes in the northern African monsoon, suggesting that improved simulation of Mediterranean climates is linked to improvements in simulating the climate of northern Africa.

Supplementary material related to this article is available online at http://www.clim-past-discuss.net/9/5347/2013/cpd-9-5347-2013-supplement.pdf.

Acknowledgements. This work was initiated when A. Perez-Sanz was a guest scientist at Macquarie University; we thank the Department of Biology for providing funds to facilitate this visit. G. Li is supported by an International Postgraduate Research Scholarship at Macquarie University. This research was supported by the Australian Research Council, grant number DP1201100343 (SPH) and the CGL2012-33063 (PGS) by the Spanish CICYT. We acknowledge the World Climate Research Programme's Working Group on Coupled Modelling, which is responsible for CMIP, and the climate modeling groups for producing and making available their model output. (For CMIP the US Department of Energy's Program for Climate Model Diagnosis and Intercomparison provides coordinating support and led development of software infrastructure in partnership with the Global Organization for Earth System Science Portals). The analyses and figures are based on data archived at CMIP5 on 15 August 2012.

References

Amatulli, G., Camia, A., and San-Miguel-Ayanz, J.: Estimating future burned areas under changing climate in the EU-Mediterranean countries, Sci. Total Environ., 450–451, 209–222, doi:10.1016/j.scitotenv.2013.02.014, 2013.

Bartlein, P. J., Harrison, S. P., Brewer, S., Connor, S., Davis, B. A. S., Gajewski, K., Guiot, J., Harrison-Prentice, T. I., Henderson, A., Peyron, O., Prentice, I. C., Scholze, M., Seppä, H., Shuman, B., Sugita, S., Thompson, R. S., Viau, A. E., Williams, J., and Wu, H.: Pollen-based continental climate reconstructions at 6 and 21 ka: a global synthesis, Clim. Dynam., 37, 775–802, doi:10.1007/s00382-010-0904-1, 2011.

Bonfils, C., de Noblet-Ducoudré, N., Guiot, J., and Bartlein, P.: Some mechanisms of mid-Holocene climate change in Europe, inferred from comparing PMIP models to data, Clim. Dynam., 23, 79–98, doi:10.1007/s00382-004-0425-x, 2004.

Bosmans, J. H. C., Drijfhout, S. S., Tuenter, E., Lourens, L. J., Hilgen, F. J., and Weber, S. L.: Monsoonal response to mid-holocene orbital forcing in a high resolution GCM, Clim. Past, 8, 723–740, doi:10.5194/cp-8-723-2012, 2012.

Braconnot, P., Loutre, M., Dong, B., Joussaume, S., and Valdes, P.: How the simulated change in monsoon at 6 ka BP is related to the simulation of the modern climate: results from the Paleoclimate Modeling Intercomparison Project, Clim. Dynam., 19, 107–121, doi:10.1007/s00382-001-0217-5, 2002.

Braconnot, P., Otto-Bliesner, B., Harrison, S., Joussaume, S., Peterchmitt, J.-Y., Abe-Ouchi, A., Crucifix, M., Driesschaert, E., Fichefet, Th., Hewitt, C. D., Kageyama, M., Kitoh, A., Laîné, A., Loutre, M.-F., Marti, O., Merkel, U., Ramstein, G., Valdes, P., Weber, S. L., Yu, Y., and Zhao, Y.: Results of PMIP2 coupled simulations of the Mid-Holocene and Last Glacial Maximum – Part 1: experiments and large-scale features, Clim. Past, 3, 261–277, doi:10.5194/cp-3-261-2007, 2007a.

Braconnot, P., Otto-Bliesner, B., Harrison, S., Joussaume, S., Peterchmitt, J.-Y., Abe-Ouchi, A., Crucifix, M., Driesschaert, E., Fichefet, Th., Hewitt, C. D., Kageyama, M., Kitoh, A., Loutre, M.-F., Marti, O., Merkel, U., Ramstein, G., Valdes, P., Weber, L., Yu, Y., and Zhao, Y.: Results of PMIP2 coupled simulations of the Mid-Holocene and Last Glacial Maximum – Part 2: feedbacks with emphasis on the location of the ITCZ and mid- and high latitudes heat budget, Clim. Past, 3, 279–296, doi:10.5194/cp-3-279-2007, 2007b.

Braconnot, P., Harrison, S. P., Kageyama, M., Bartlein, P. J., Masson-Delmotte, V., Abe-Ouchi, A., Otto-Bliesner, B., and Zhao, Y.: Evaluation of climate models using palaeoclimatic data, Nat. Clim. Change, 2, 417–424, doi:10.1038/nclimate1456, 2012.

Brands, S., Herrera, S., Fernández, J., and Gutiérrez, J. M.: How well do CMIP5 Earth System Models simulate present climate conditions in Europe and Africa?: A performance comparison for the downscaling community, Clim. Dynam., 41, 803–817, doi:10.1007/s00382-013-1742-8, 2013.

Brayshaw, D. J., Rambeau, C. M. C. and Smith, S. J.: Changes in Mediterranean climate during the Holocene: Insights from global and regional climate modelling, Holocene, 21, 15–31, doi:10.1177/0959683610377528, 2011.

Brewer, S., Guiot, J., and Torre, F.: Mid-Holocene climate change in Europe: a data-model comparison, Clim. Past, 3, 499–512, doi:10.5194/cp-3-499-2007, 2007.

Camuffo, D., Bertolin, C., Barriendos, M., Dominguez-Castro, F., Cocheo, C., Enzi, S., Sghedoni, M., Valle, A., Garnier, E., Alcoforado, M. J., Xoplaki, E., Luterbacher, J., Diodato, N.,

Maugeri, M., Nunes, M. F., and Rodriguez, R.: 500-years temperatura reconstruction in the Mediterranean Basin by means of documentary data and instrumental observations, Climatic Change, 101, 169–199, 2010.

Carrión, J. S., Fernández, S., González-Sampériz, P., Gil-Romera, G., Badal, E., Carrión-Marco, Y., López-Merino, L., López-Sáez, J. A., Fierro, E., and Burjachs, F.: Expected trends and surprises in the Lateglacial and Holocene vegetation history of the Iberian Peninsula and Balearic Islands, Rev. Palaeobot. Palynol., 162, 458–475, doi:10.1016/j.revpalbo.2009.12.007, 2010.

Cheddadi, R., Yu, G., Guiot, J., Harrison, S. P., and Prentice, I. C.: The climate of Europe 6000 years ago, Clim. Dynam., 13, 1–9, doi:10.1007/s003820050148, 1997.

CLIVAR – Climate in Spain: Past, Present and Future, in: Regional climate change assessment report, edited by: Pérez, F. F. and Boscolo, R., Ministerio de Ciencia e Innovación, Madrid, 83 pp., 2010.

Coe, M. T. and Harrison, S. P.: The water balance of northern Africa during the mid-Holocene: an evaluation of the 6 ka BP PMIP simulations, Clim. Dynam., 19, 155–166, doi:10.1007/s00382-001-0219-3, 2002.

Davis, B. A. S., Brewer, S., Stevenson, A. C., and Guiot, J.: The temperature of Europe during the Holocene reconstructed from pollen data, Quaternary Sci. Rev., 22, 1701–1716, doi:10.1016/S0277-3791(03)00173-2, 2003.

Dunne, J., Evershed, R. P., Salque, M., Cramp, L., Bruni, S., Ryan, K., Biagetti, S., and di Lernia, S.: First dairying in green Saharan Africa in the fifth millennium bc, Nature, 486, 390–394, doi:10.1038/nature11186, 2012.

European Environment Agency: Climate change, impacts and vulnerability in Europe 2012: an indicator-based report, European Environment Agency, Copenhagen, 2012.

Forman, S. L., Oglesby, R., Markgraf, V., and Stafford, T.: Paleoclimatic significance of Late Quaternary eolian deposition on the Piedmont and High Plains, Central United States, Global Planet. Change, 11, 35–55, doi:10.1016/0921-8181(94)00015-6, 1995.

Gaetani, M., Pohl, B., Douville, H., and Fontaine, B.: West African Monsoon influence on the summer Euro-Atlantic circulation, Geophys. Res. Lett., 38, L09705, doi:10.1029/2011GL047150, 2011.

Giorgi, F.: Climate change hot-spots, Geophys. Res. Lett., 33, L08707, doi:10.1029/2006GL025734, 2006.

Giorgi, F. and Lionello, P.: Climate change projections for the Mediterranean region, Global Planet. Change, 63, 90–104, doi:10.1016/j.gloplacha.2007.09.005, 2008.

Guiot, J., Boreux, J. J., Braconnot, P., and Torre, F.: Data-model comparison using fuzzy logic in paleoclimatology, Clim. Dynam., 15, 569–581, doi:10.1007/s003820050301, 1999.

Haerter, J. O., Hagemann, S., Moseley, C., and Piani, C.: Climate model bias correction and the role of timescales, Hydrol. Earth Syst. Sci., 15, 1065–1079, doi:10.5194/hess-15-1065-2011, 2011.

Harris, I., Jones, P. D., Osborn, T. J., and Lister, D. H.: Updated high-resolution grids of monthly climatic observations – the CRU TS3.10 Dataset, Int. J. Climatol., doi:10.1002/joc.3711, in press, 2013.

Harrison, S. P., Prentice, I. C., and Bartlein, P. J.: Influence of insolation and glaciation on atmospheric circulation in the North Atlantic sector: Implications of general circulation model experiments for the Late Quaternary climatology of Europe, Quaternary Sci. Rev., 11, 283–299, doi:10.1016/0277-3791(92)90002-P, 1992.

Harrison, S. P., Bartlein, P. J., Brewer, S., Prentice, I. C., Boyd, M., Hessler, I., Holmgren, K., Izumi, K., and Willis, K.: Model benchmarking with glacial and mid-Holocene climates, Clim. Dynam., doi:10.1007/s00382-013-1922-6, in press, 2013.

Hoelzmann, P., Jolly, D., Harrison, S. P., Laarif, F., Bonnefille, R., and Pachur, H.-J.: Mid-Holocene land-surface conditions in northern Africa and the Arabian Peninsula: A data set for the analysis of biogeophysical feedbacks in the climate system, Glob. Biogeochem. Cy, 12, 35–51, doi:10.1029/97GB02733, 1998.

Hoerling, M., Eischeid, J., Perlwitz, J., Quan, X., Zhang, T., and Pegion, P.: On the increased frequency of Mediterranean drought, J. Climate, 25, 2146–2161, 2012.

Ibanez, F.: Sur une nouvelle application de la théorie de 1'information à la description des séries chronologiques planctoniques, J. Plankton Res., 4, 619–632, doi:10.1093/plankt/4.3.619, 1982.

Izumi, K., Bartlein, P. J., and Harrison, S. P.: Consistent large-scale temperature responses in warm and cold climates, Geophys. Res. Lett., 40, 1817–1823, doi:10.1002/grl.50350, 2013.

Joussaume, S., Taylor, K. E., Braconnot, P., Mitchell, J. F. B., Kutzbach, J. E., Harrison, S. P., Prentice, I. C., Broccoli, A. J., Abe-Ouchi, A., Bartlein, P. J., Bonfils, C., Dong, B., Guiot, J., Herterich, K., Hewitt, C. D., Jolly, D., Kim, J. W., Kislov, A., Kitoh, A., Loutre, M. F., Masson, V., McAvaney, B., McFarlane, N., de Noblet, N., Peltier, W. R., Peterschmitt, J. Y., Pollard, D., Rind, D., Royer, J. F., Schlesinger, M. E., Syktus, J., Thompson, S., Valdes, P., Vettoretti, G.,

Webb, R. S., and Wyputta, U.: Monsoon changes for 6000 years ago: Results of 18 simulations from the Paleoclimate Modeling Intercomparison Project (PMIP), Geophys. Res. Lett., 26, 859–862, doi:10.1029/1999GL900126, 1999.

Kelley, C., Ting, M., Seager, R., and Kushnir, Y.: Mediterranean precipitation climatology, seasonal cycle, and trend as simulated by CMIP5, Geophys. Res. Lett., 39, L21703, doi:10.1029/2012GL053416, 2012.

Kelley, D. I., Prentice, I. C., Harrison, S. P., Wang, H., Simard, M., Fisher, J. B., and Willis, K. O.: A comprehensive benchmarking system for evaluating global vegetation models, Biogeosciences, 10, 3313–3340, doi:10.5194/bg-10-3313-2013, 2013.

Kohfeld, K. E. and Harrison, S. P.: How well can we simulate past climates? Evaluating the models using global palaeoenvironmental datasets, Quaternary Sci. Rev., 19, 321–346, doi:10.1016/S0277-3791(99)00068-2, 2000.

Kuper, R. and Kröpelin, S.: Climate-Controlled Holocene Occupation in the Sahara: Motor of Africa's Evolution, Science, 313, 803–807, doi:10.1126/science.1130989, 2006.

Levis, S., Bonan, G. B., and Bonfils, C.: Soil feedback drives the mid-Holocene North African monsoon northward in fully coupled CCSM2 simulations with a dynamic vegetation model, Clim. Dynam., 23, 791–802, doi:10.1007/s00382-004-0477-y, 2004.

Li, G., Harrison, S. P., Bartlein, P. J., Izumi, K., and Colin Prentice, I.: Precipitation scaling with temperature in warm and cold climates: An analysis of CMIP5 simulations, Geophys. Res. Lett., 40, 4018–4024, doi:10.1002/grl.50730, 2013.

Lionello, P.: The climate of the Mediterranean Region from the past to the future, Elsevier Science, Burlington, 2012.

Luterbacher, J., Xoplaki, E., Casty, C., Wanner, H., Pauling, A., Kuttel, M., Rutishauser, T., Bronnimann, S., Fischer, E., and Fleitmann, D.: Chapter 1 Mediterranean climate variability over the last centuries: A review, in Developments in Earth and Environmental Sciences, 4, Elsevier, 27–148, 2006.

Magny, M., Miramont, C., and Sivan, O.: Assessment of the impact of climate and anthropogenic factors on Holocene Mediterranean vegetation in Europe on the basis of palaeohydrological records, Palaeogeogr. Palaeocl., 186, 47–59, doi:10.1016/S0031-0182(02)00442-X, 2002.

Marzin, C. and Braconnot, P.: Variations of Indian and African monsoons induced by insolation changes at 6 and 9.5 kyr BP, Clim. Dynam., 33, 215–231, doi:10.1007/s00382-009-0538-3, 2009.

Masson, V., Cheddadi, R., Braconnot, P., Joussaume, S., and Texier, D.: Mid-Holocene climate in Europe: what can we infer from PMIP model-data comparisons?, Clim. Dynam., 15, 163–182, doi:10.1007/s003820050275, 1999.

Meehl, G. A., Stocker, T. F., Collins, W. D., Friedlingstein, P., Gaye, A. T., Gregory, J. M., Kitoh, A., Knutti, R., Murphy, J. M., Nodas, A., Raper, S. C. B., Watterson, I. G., Weaver, A. J., and Zhao, Z. C.: Global Climate Projections, in: Climate Change 2007: The Physical Science Basis. Contribution of Working Group I to the Fourth Assessment Report of the Intergovernmental Panel on Climate Change, edited by: Solomon, S., Quin, D., Manning, M., Chen, Z., Marquis, M., Averyt, K. B., Tignor, M., and Miller, H. L., Cambridge University Press, Cambridge, UK and New York, USA, 2007.

Mehta, A. V. and Yang, S.: Precipitation climatology over Mediterranean Basin from ten years of TRMM measurements, Adv. Geosci., 17, 87–91, doi:10.5194/adgeo-17-87-2008, 2008.

Monerie, P.-A., Fontaine, B., and Roucou, P.: Expected future changes in the African monsoon between 2030 and 2070 using some CMIP3 and CMIP5 models under a medium-low RCP scenario, J. Geophys. Res., 117, doi:10.1029/2012JD017510, 2012.

Moreira, F., Viedma, O., Arianoutsou, M., Curt, T., Koutsias, N., Rigolot, E., Barbati, A., Corona, P., Vaz, P., Xanthopoulos, G., Mouillot, F., and Bilgili, E.: Landscape – wildfire interactions in southern Europe: Implications for landscape management, J. Environ. Manage., 92, 2389–2402, doi:10.1016/j.jenvman.2011.06.028, 2011.

Niedermeyer, E. M., Schefuß, E., Sessions, A. L., Mulitza, S., Mollenhauer, G., Schulz, M., and Wefer, G.: Orbital- and millennial-scale changes in the hydrologic cycle and vegetation in the western African Sahel: insights from individual plant wax δD and δ^{13}C, Quaternary Sci. Rev., 29, 2996–3005, doi:10.1016/j.quascirev.2010.06.039, 2010.

Nikulin, G., Kjellström, E., Hansson, U., Strandberg, G., and Ullerstig, A.: Evaluation and future projections of temperature, precipitation and wind extremes over Europe in an ensemble of regional climate simulations, Tellus, 63, 41–55, doi:10.1111/j.1600-0870.2010.00466.x, 2011.

Prentice, C., Guiot, J., Huntley, B., Jolly, D., and Cheddadi, R.: Reconstructing biomes from palaeoecological data: a general method and its application to European pollen data at 0 and 6 ka, Clim. Dynam., 12, 185–194, doi:10.1007/BF00211617, 1996.

Prentice, I. C. and Jolly, D.: Mid-Holocene and glacial-maximum vegetation geography of the northern continents and Africa, J. Biogeogr., 27, 507–519, doi:10.1046/j.1365-2699.2000.00425.x, 2000.

Raicich, F., Pinardi, N., and Navarra, A.: Teleconnections between Indian monsoon and Sahel rainfall and the Mediterranean, Int. J. Climatol., 23, 173–186, doi:10.1002/joc.862, 2003.

Roberts, N., Stevenson, T., Davis, B., Cheddadi, R., Brewster, S., and Rosen, A.: Holocene climate, environment and cultural change in the circum-Mediterranean region, in: Past Climate Variability through Europe and Africa, vol. 6, edited by: Battarbee, R. W., Gasse, F., and Stickley, C. E., Springer Netherlands, Dordrecht, 343–362, 2004.

Roberts, N., Jones, M. D., Benkaddour, A., Eastwood, W. J., Filippi, M. L., Frogley, M. R., Lamb, H. F., Leng, M. J., Reed, J. M., Stein, M., Stevens, L., Valero-Garcés, B., and Zanchetta, G.: Stable isotope records of Late Quaternary climate and hydrology from Mediterranean lakes: the ISOMED synthesis, Quaternary Sci. Rev., 27, 2426–2441, doi:10.1016/j.quascirev.2008.09.005, 2008.

Roberts, N., Eastwood, W. J., Kuzucuoglu, C., Fiorentino, G., and Caracuta, V.: Climatic, vegetation and cultural change in the eastern Mediterranean during the mid-Holocene environmental transition, Holocene, 21, 147–162, doi:10.1177/0959683610386819, 2011.

Rodwell, M. J. and Hoskins, B. J.: Subtropical Anticyclones and Summer Monsoons, J. Climate, 14, 3192–3211, doi:10.1175/1520-0442(2001)014<3192:SAASM>2.0.CO;2, 2001.

Roehrig, R., Bouniol, D., Guichard, F., Hourdin, F., and Redelsperger, J.-L.: The present and future of the West African monsoon: a process-oriented assessment of CMIP5 simulations along the AMMA transect, J. Climate, 26, 6471–6505, doi:10.1175/JCLI-D-12-00505.1, 2013.

Schmidt, G. A., Annan, J. D., Bartlein, P. J., Cook, B. I., Guilyardi, E., Hargreaves, J. C., Harrison, S. P., Kageyama, M., LeGrande, A. N., Konecky, B., Lovejoy, S., Mann, M. E., Masson-Delmotte, V., Risi, C., Thompson, D., Timmermann, A., Tremblay, L.-B., and Yiou, P.: Using paleo-climate comparisons to constrain future projections in CMIP5, Clim. Past Discuss., 9, 775–835, doi:10.5194/cpd-9-775-2013, 2013.

Soler, M., Serra, T., Colomer, J., and Romero, R.: Anomalous rainfall and associated atmospheric circulation in the northeast Spanish Mediterranean area and its relationship to sediment fluidization events in a lake, Water Resour. Res., 43, W01404, doi:10.1029/2005WR004810, 2007.

Sperber, K. R., Annamalai, H., Kang, I.-S., Kitoh, A., Moise, A., Turner, A., Wang, B., and Zhou, T.: The Asian summer monsoon: an intercomparison of CMIP5 vs. CMIP3 simulations of the late 20th century, Clim. Dynam., doi:10.1007/s00382-012-1607-6, in press, 2012.

Taylor, K. E., Stouffer, R. J., and Meehl, G. A.: An Overview of CMIP5 and the Experiment Design, B. Am. Meteorol. Soc., 93, 485–498, doi:10.1175/BAMS-D-11-00094.1, 2012.

Tierney, J. E., Lewis, S. C., Cook, B. I., LeGrande, A. N., and Schmidt, G. A.: Model, proxy and isotopic perspectives on the East African Humid Period, Earth Planet. Sc. Lett., 307, 103–112, doi:10.1016/j.epsl.2011.04.038, 2011.

Vanniere, B., Power, M. J., Roberts, N., Tinner, W., Carrion, J., Magny, M., Bartlein, P., Colombaroli, D., Daniau, A. L., Finsinger, W., Gil-Romera, G., Kaltenrieder, P., Pini, R., Sadori, L., Turner, R., Valsecchi, V., and Vescovi, E.: Circum-Mediterranean fire activity and climate changes during the mid-Holocene environmental transition (8500–2500 cal. BP), Holocene, 21, 53–73, doi:10.1177/0959683610384164, 2011.

van Soelen, E., Brooks, G., Larson, R., Sinninghe Damste, J., and Reichart, G.: Mid- to late-Holocene coastal environmental changes in southwest Florida, USA, Holocene, 22, 929–938, doi:10.1177/0959683611434226, 2012.

Watrin, J., Lézine, A.-M., and Hély, C.: Plant migration and plant communities at the time of the "green Sahara", C. R. Geosci., 341, 656–670, doi:10.1016/j.crte.2009.06.007, 2009.

Wohlfahrt, J., Harrison, S. P., and Braconnot, P.: Synergistic feedbacks between ocean and vegetation on mid- and high-latitude climates during the mid-Holocene, Clim. Dynam., 22, 223–238, doi:10.1007/s00382-003-0379-4, 2004.

Xoplaki, E., González-Rouco, F., Luter, J., and Wanner, H.: Mediterranean summer air temperature variability and its connection to the large-scale atmospheric circulation and SSTs, Clim. Dynam., 20, 723–739, 2003.

Zhao, Y. and Harrison, S. P.: Mid-Holocene monsoons: a multi-model analysis of the inter-hemispheric differences in the responses to orbital forcing and ocean feedbacks, Clim. Dynam., 39, 1457–1487, doi:10.1007/s00382-011-1193-z, 2011.

Table 1. Characteristics of the CMIP5 models used in these analyses.

Model name	Type	Resolution (number of gridcells: latitude, longitude)			Year length	Simulations		
		Atmosphere	Ocean	Sea Ice		*midHolocene*	*piControl*	*historical*
BCC-CSM1-1	OAC	64, 128	232, 360	232, 360	365	X	X	
CCSM4	OA	192, 288	320, 384	320, 384	365	X	X	X
CNRM-CM5	OA	128, 256	292, 362	292, 362	365–366	X	X	
CSIRO-Mk3-6-0	OA	96, 192	189, 192	96, 192	365	X	X	
CSIRO-Mk3L-1-2	OA	56, 64	128, 225	56, 64	365	X	X	
GISS-E2-R	OA	90, 144	90, 144	90, 144	365	X	X	X
HadGEM2-CC	OAC	145, 192	216, 360	216, 360	360	X	X	
HadGEM2-ES	OAC	145, 192	216, 360	216, 360	360	X	X	
IPSL-CM5A-LR	OAC	96, 96	149, 182	149, 182	365	X	X	X
MIROC-ESM	OAC	64, 128	192, 256	192, 256	365	X	X	X
MPI-ESM-P	OA	96, 192	220, 256	220, 256	365–366	X	X	X
MRI-CGCM3	OA	160, 320	360, 368	360, 368	365	X	X	X

Table 2. Summary of area-averaged climate anomalies (*midHolocene* – *piControl*) for individual models for individual seasons and for mean annual precipitation. Bold font indicates significant values. The seasons are spring: March, April, May; summer: June, July, August; autumn: September, October, November; winter: December, January, February.

	Season anomaly	BCC-CSM1.1	CCSM4	CNRM-CM5	CSIRO-Mk3-6-0	CSIRO-Mk3L-1-2	GISS-E2-R	HadGEM2-CC	HadGEM2-ES	IPSL-CM5A-LR	MIROC-ESM	MPI-ESM-P	MRI-CGCM3
Mediterranean	annual	15.0	24.4	32.6	−21.2	8.4	**75.7**	30.9	9.2	40.1	30.8	14.3	15.4
	spring	13.9	3.7	16.1	13.0	4.2	**28.4**	14.5	13.0	22.2	11.6	17.6	10.4
	summer	−4.3	2.7	4.7	−10.7	−2.4	20.5	**40.6**	−8.8	14.0	0.8	3.5	−2.8
	autumn	−0.4	10.5	14.0	−21.6	6.6	20.3	**−40.9**	2.9	8.0	6.0	−3.9	−5.9
	winter	5.8	7.4	−2.3	−1.9	0.0	6.5	16.7	2.1	−4.1	12.4	−2.9	13.8
Desert	annual	7.7	**29.5**	**32.7**	−18.5	4.6	**22.8**	4.5	4.4	**6.8**	**26.1**	**14.3**	7.7
	spring	0.1	0.6	3.6	0.8	1.3	10.6	0.6	2.1	**1.8**	4.2	2.1	0.1
	summer	0.8	**14.3**	**9.6**	−7.4	**3.2**	7.7	**3.4**	**4.2**	**2.8**	**12.3**	**6.7**	0.8
	autumn	2.8	**13.9**	**18.5**	−11.5	0.9	3.9	2.1	−1.3	**2.3**	**10.1**	**5.1**	2.8
	winter	4.1	0.6	1.0	−0.5	−0.8	0.7	−1.7	−0.5	−0.1	−0.4	0.4	4.1
Monsoon	annual	**47.4**	**148.6**	**155.8**	−53.5	**47.2**	**116.1**	**207.6**	**210.4**	**202.4**	**182.1**	**219.9**	**88.5**
	spring	−11.2	−2.6	−7.4	−2.6	−2.7	−7.5	**−39.1**	**19.3**	6.0	−19.7	**17.5**	−1.9
	summer	**33.6**	**80.4**	**97.2**	−20.3	**21.5**	**91.6**	15.4	**122.8**	**110.0**	**142.4**	**132.8**	**68.3**
	autumn	**29.8**	**76.6**	**78.7**	−28.3	**32.9**	**41.4**	**233.6**	**72.5**	**89.6**	**72.2**	**70.2**	**23.7**
	winter	−4.7	−5.9	**−12.6**	−2.3	**−4.5**	**−9.4**	−2.2	−4.3	**−3.2**	**−12.7**	−0.7	−1.5
DP	annual	−76.7	−13.3	–	**−208.8**	−36.4	2.8	**123.0**	**142.0**	–	**−244.4**	14.3	–
	spring	−41.3	0.5	–	−12.7	−0.6	**−56.2**	**−100.9**	−1.7	–	**−87.2**	−32.0	–
	summer	1.1	43.8	–	**−68.1**	33.9	**87.1**	−1.8	8.6	–	29.3	38.7	–
	autumn	29.1	53.1	–	**−106.8**	**63.2**	**71.0**	**154.9**	**168.9**	–	−9.6	**55.6**	–
	winter	**−65.5**	**−110.7**	–	−21.1	**−132.9**	**−99.1**	**70.7**	**−33.9**	–	**−176.9**	**−48.1**	–

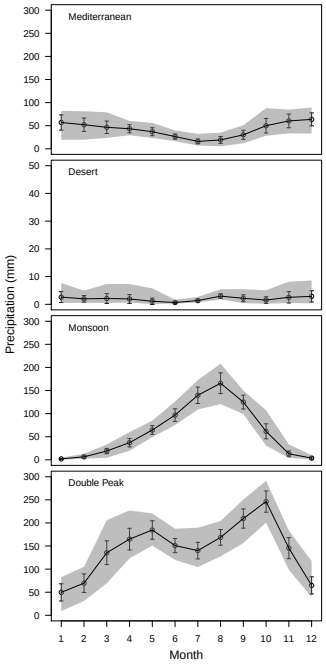

Fig. 1. Observed seasonal cycle of precipitation in each of the defined climate zones, using the CRU T3.1 data set (Harris et al., 2013). The mean precipitation each month (mm) is shown by the black line, with the standard deviation shown by the bars. The grey shading shows the maximum and minimum rainfall experienced within the observation period (1961–1990). Note that the scale for the desert region differs from that used for the other regions. Months are numbered consecutively from January (1) through to December (12).

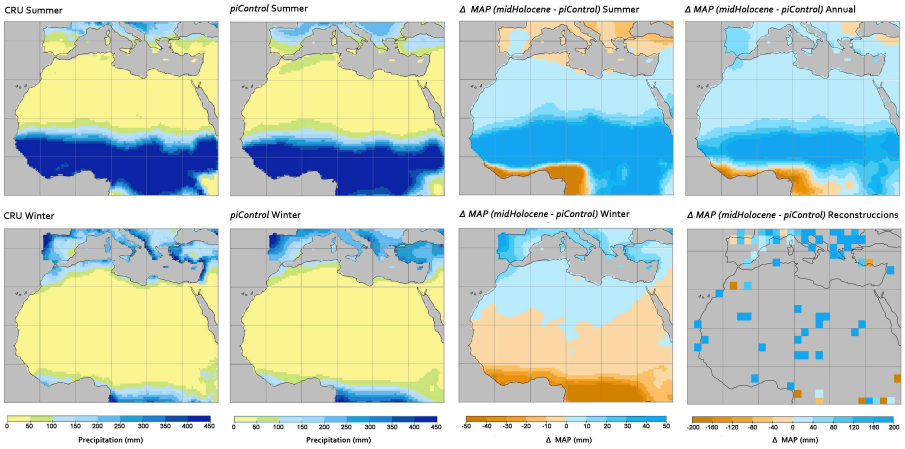

Fig. 2. Observed and simulated modern and palaeo-precipitation patterns. The total summer (June, July, August) and winter (December, January, February) precipitation from the CRU T3.1 data set (Harris et al., 2013) are compared to ensemble averages of the *piControl* outputs of the 12 CMIP5 models. The simulated change in precipitation between the Mid-Holocene and *piControl* simulations (*midHolocene – piControl*) is shown based on the ensemble average of the *midHolocene* outputs of the 12 CMIP5 models. The observed anomalies in mean annual precipitation (MAP) between the mid-Holocene and the present day are average values for $2 \times 2^{\circ}$ grids from the Bartlein et al. (2011) data set.

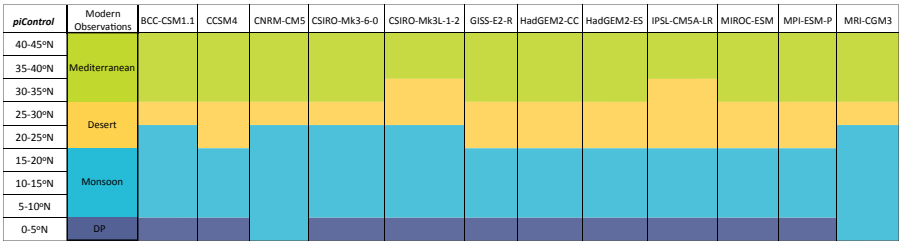

Fig. 3. The location of the four precipitation zones in the CMIP5 pre-industrial (*piControl*) simulations compared to the limits defined using the CRU TS3.1 data set (Harris et al., 2013). The precipitation regime was characterised using zonally-averaged long-term means for 5° latitiude bands.

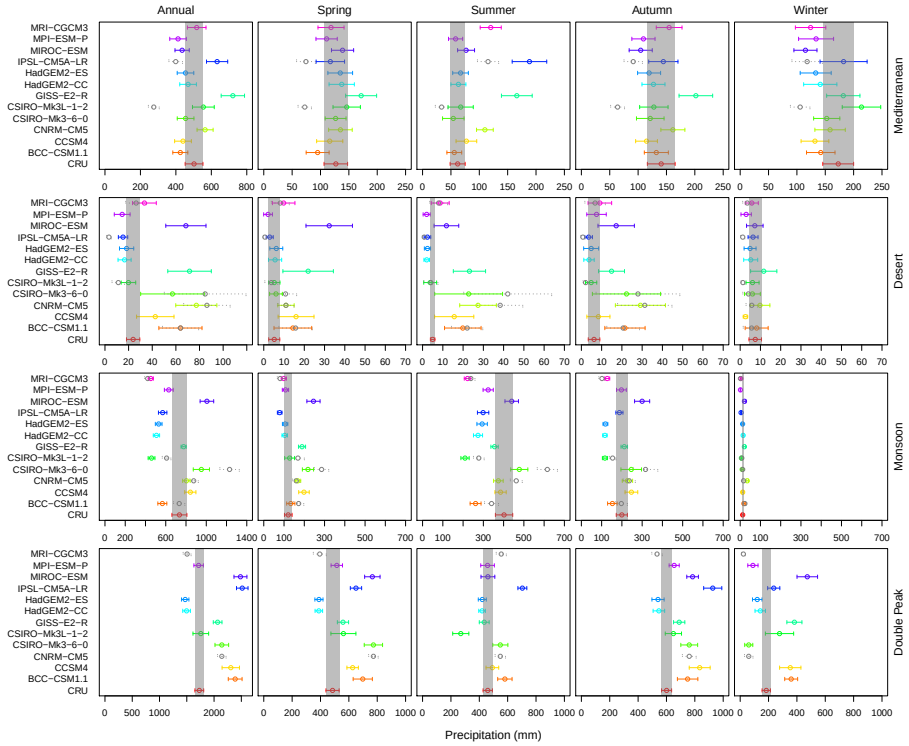

5381

Fig. 4. Comparison of simulated and observed mean annual and mean seasonal precipitation (mm) for each of the defined precipitation regimes (Mediterranean, desert, monsoon, double peak). The simulated precipitation (mean and standard deviation) is shown for both the climate zone as defined by the observations (solid line) and as defined in the *piControl* simulation itself (dotted line). The difference between these two lines for each model provides a measure of the degree to which incorrect placement of a given climate affects the zonal means. The grey bars represent one standard deviation of the mean annual and mean seasonal precipitation from observations. The seasons are defined as spring (March, April, May), summer (June, July, August), autumn (September, October, November) and winter (December, January, February).

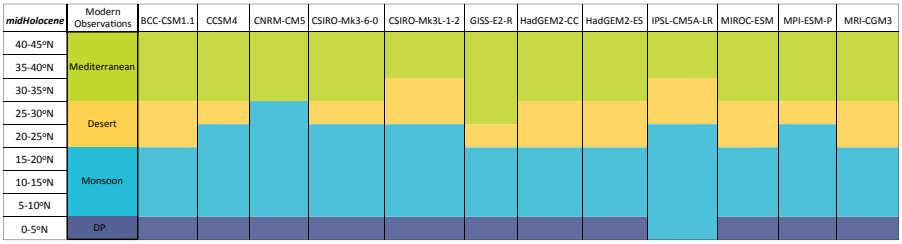

Fig. 5. The location of the four precipitation zones in the CMIP5 mid-Holocene (*midHolocene*) simulations compared to the limits defined using the CRU TS3.1 data set (Harris et al., 2013). The precipitation regime was characterised using zonally-averaged long-term means for 5° latitude bands.

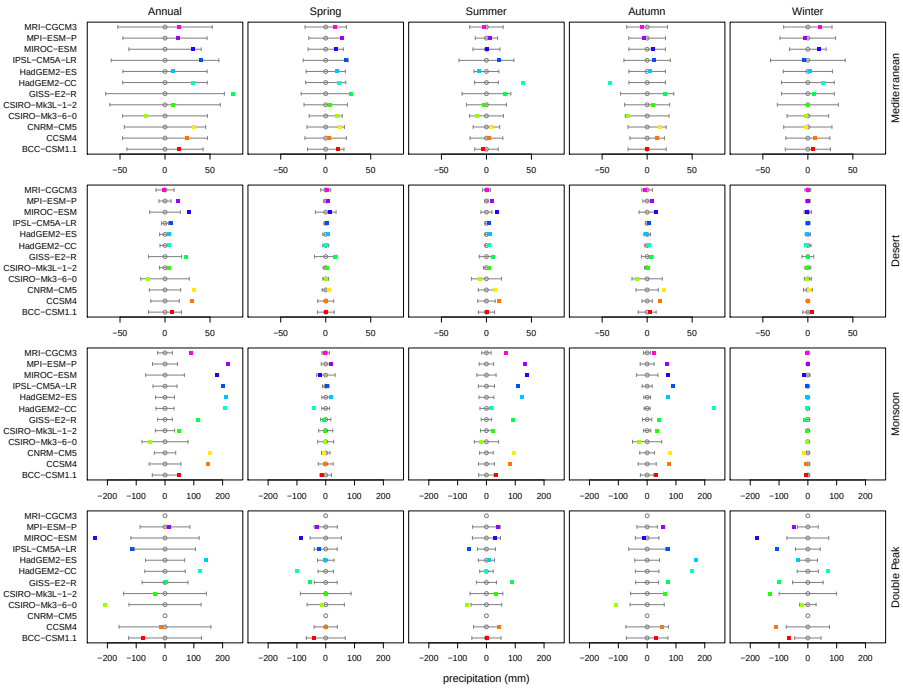

Fig. 6. Simulated changes in total and seasonal precipitation in the mid-Holocene (*mid-Holocene*) compared to the pre-industrial control (*piControl*) for each of the four precipitation regimes (Mediterranean, desert, monsoon, double peak) for the region that is common between the two sets of simulations. The standard deviation of precipitation in the *piControl* control simulation of each model is shown (grey bars) to provide a visual measure of the significance of the simulated change in precipitation. The seasons are defined as spring (March, April, May), summer (June, July, August), autumn (September, October, November) and winter (December, January, February).

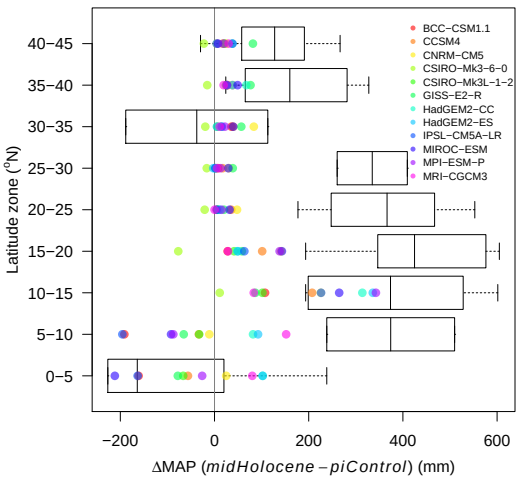

Fig. 7. Comparison of simulated and reconstructed changes in mean annual precipitation in the mid-Holocene for 5° latitude bands between 0 and 45° N. The reconstructions are from the Bartlein et al. (2011) data set. The mean, 25–75 % range and full range of the reconstructions are shown (for those latitude bands with sufficient data points). The model results are averages for the grid cells with observations.

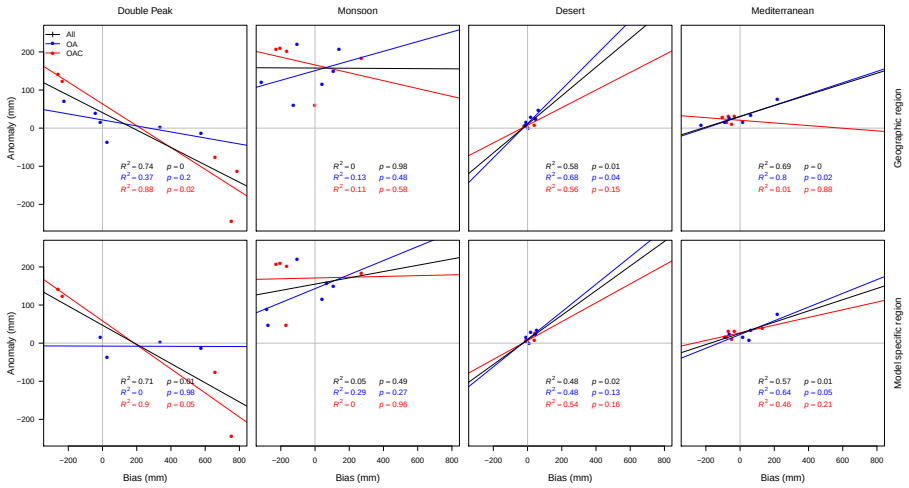

Fig. 8. Relationship between biases in the *piControl* simulation of mean annual precipitation (mm) and mid-Holocene precipitation anomalies (*midHolocene – piControl*) as simulated by each of the CMIP5 models for each of the precipitation regimes (Double Peak, Monsoon, Desert, Mediterranean). The upper panels show biases and anomalies calculated for specific latitudinal bands as defined from the modern observed spatial extent of each regime (geographic region). The lower panels show biases and anomalies calculated for the region identified as characterized by a given regime in each model and simulation (model specific region). The regressions are calculated for all models (all: black), for the coupled ocean-atmosphere models (OA: blue) and for the carbon-cycle models (OAC: red).

5387

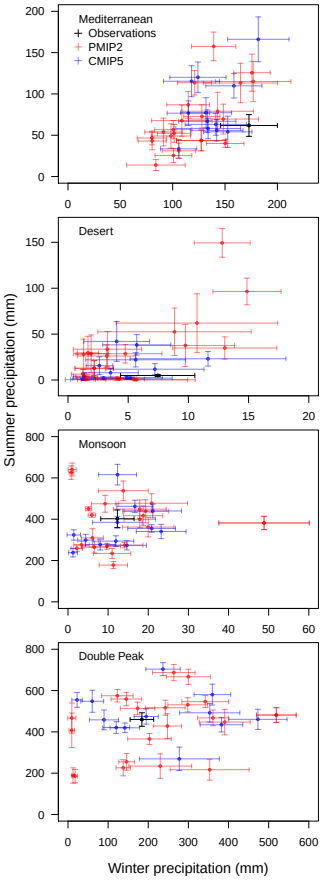

5388

Fig. 9. Comparison of simulated and observed summer and winter precipitation in each of the four precipitation regimes (Mediterranean, Desert, Monsoon, Double Peak). The observations (black) are the average for the period 1961–1990 from the CRU T3.1 data set (Harris et al., 2013). The simulated mean and standard deviation of precipitation from the CMIP5 models (blue) is based on the last 100 yr of the *piControl*. These simulations can be compared with results from coupled ocean-atmosphere simulations made during the second phase of the Palaeoclimate Modelling Intercomparison Project (PMIP2: Braconnot et al., 2012; shown in red). The PMIP2 results are the mean and standard deviation based on the last 100 yr of a *piControl*, except in three cases where only 50 yr of data were available. Model results are calculated for each precipitation regime based on the observed geographic extent characterized by these regimes, as defined using the CRU TS3.1 data set. Summer is defined as June, July, and August; winter is December, January, February.